Recovering Channel Amplitude Reciprocity with Data-Aided Gain Imbalance Estimation in an SFLC-OFDM System

Songmin Lee
Department of Electrical Engineering
Sookmyung Women's University
Seoul, South Korea
lsm0723@sookmyung.ac.kr

Jingon Joung
School of Electrical and Electronics Engineering
Chung-Ang University
Seoul, South Korea
jgjoung@cau.ac.kr

Jihoon Choi
School of Electronics and Information Engineering
Korea Aerospace University
Seoul, South Korea
jihoon@kau.ac.kr

Juyeop Kim
Department of Electrical Engineering
Sookmyung Women's University
Seoul, South Korea
jykim@sookmyung.ac.kr

***Abstract*—This paper proposes a practical scheme for estimating and compensating channel amplitude asymmetry in a Space-Frequency Line Code (SFLC) - Orthogonal Frequency Division Multiplexing (OFDM) system. SFLC assumes channel reciprocity using Time Division Duplexing (TDD) for estimating downlink (DL) channel state information via uplink (UL). However, in practice, channel amplitudes between UL and DL are asymmetric, causing unexpected phase rotation in decoded symbols. To address the issue, we propose a data-aided gain calibration technique to maintain channel amplitude symmetry and improve the performance of SFLC decoding. We design an estimator of the phase rotation based on a mathematical model. We then propose a calibration scheme that compensates for channel amplitude asymmetry by adjusting the receive gain of an antenna. We also provide experimental results with implementation on a software modem. A testbed using USRPs is established, and experiments with real-time signal processing are conducted to verify the functionality. The results show that the phase rotation is properly estimated and effectively nullified via the proposed scheme.**

***Index Terms*—gain calibration, space-frequency line code, channel reciprocity, software modem, channel amplitude asymmetry**

I. Introduction

Mobile communications have taken a step forward into their next generation by employing a game-changing technology. For the past decades, it has benefited from Orthogonal Frequency Division Multiplexing (OFDM), which offers the freedom of signal transmission in the frequency domain. Recent systems aim to achieve a similar evolution in the space domain by utilizing Multiple Input and Multiple Output (MIMO) technology, which can generate multiple data streams through spatial characteristics [1], [2]. These key technologies enable mobile communications to offer enhanced capacity and can be applied to various use cases, including military applications.

To further achieve flexibility in the spatial domain, recent MIMO technologies have advanced to multiplex the data of multiple users with massive antenna arrays [3]. These technologies typically rely on Channel State Information at Transmitter (CSIT) for a sophisticated precoding process based on the channel state. The challenge of CSIT realization is conventionally addressed by utilizing feedback of the estimated channel at the receiver, but this approach is reaching its limit. Channel state feedback inherently involves quantization errors, which can increase the Error Vector Magnitude (EVM) of transmitted signals. Pilot overhead is another critical issue because the number of pilot transmissions is proportional to the number of transmit antennas [4].

Instead of channel state feedback, many research works jointly consider utilizing channel reciprocity with recent MIMO technologies to achieve CSIT [5]–[7]. The wireless channel is known to exhibit symmetric characteristics in a Time Division Duplexing (TDD) system, where the same frequency is utilized for bidirectional communications. Based on channel reciprocity, a transmitter can theoretically estimate the channel from received sounding signals sent by a receiver [8]. This estimation method is promising as it avoids the fundamental issues associated with channel feedback methods. Channels directly estimated with received signals are free from the quantization errors. Moreover, pilot overhead will not be a concern even in environments with massive transmit antennas, as the number of mobile antennas remains limited.

Several research works have traditionally studied channel reciprocity. Channel reciprocity with hardware imbalance is

This research was supported by Institute of Information & communications Technology Planning & Evaluation (IITP) grants funded by the Korea government(MSIT) (No. 2021-0-00874, Development of Next Generation Wireless Access Technology Based on Space Time Line Code and No. 2021-0-00165, Development of 5G+ Intelligent Base Station Software Modem).

comprehensively observed through experiments, and relative calibration methods that can achieve baseband-to-baseband reciprocity are proposed [9]–[11]. Some methods are also proposed to conduct relative calibration over-the-air without extra hardware [12], [13]. The relative calibration is further enhanced to achieve channel reciprocity based on Minimum Mean Square Error (MMSE) [14]. Many research works also considered utilizing channel reciprocity for MIMO channel estimation. A practical relative calibration scheme is jointly proposed with beamforming precoding algorithms [15]. Efficient antenna calibration methods are also proposed in network MIMO systems [16]–[19].

Despite past research on channel reciprocity, it remains challenging to utilize channel reciprocity for channel estimation in OFDM systems. The channel experienced in the frequency domain sensitively depends on the baseband-level receiving status and may not be reciprocal due to different baseband signal processing. Conventional research addresses the issue of asymmetric channel phase due to different time and frequency synchronization statuses [20]. It proposes a strict synchronization scheme to recover channel phase reciprocity and demonstrates how reciprocal channel phase can be achieved in practical environments. On the other hand, the channel reciprocity in terms of amplitude can also be distorted due to receiver gain configuration in RF chains. MIMO precoding based on CSIT will generate more EVM and cause more errors unless channel amplitude reciprocity is recovered.

In this paper, we address the issue of recovering channel amplitude reciprocity to enable more precise MIMO precoding based on CSIT. We consider this issue in terms of Space-Time Line Code (STLC), which is one of the key MIMO technologies and is extensible to massive transmit antennas [21], [22]. The novelty of this paper can be summarized as follows:

- An intensive mathematical analysis of how channel amplitude reciprocity impacts the performance of STLC decoding is provided.
- Based on the above analysis, novel amplitude imbalance estimation and gain calibration schemes, which jointly achieve precise channel amplitude reciprocity, are proposed.
- For practical assessment, the proposed schemes are implemented on a testbed and verified to demonstrate how they can resolve the imbalance issue in signal emission environments.

II. System and Channel Asymmetry Model

A. SFLC Channel Model and Frame Structure

We consider a 1x2 SFLC-OFDM system with one antenna at the transmitter (TX) and two antennas at the receiver (RX), as illustrated in Fig. 1. We denote transmissions from TX to RX as downlink (DL) and transmissions from RX to TX as uplink (UL). To address the issue where the amplitude of the channel is distorted due to the characteristics of the RF chain, we use the mathematical channel model depicted in Fig. 1.

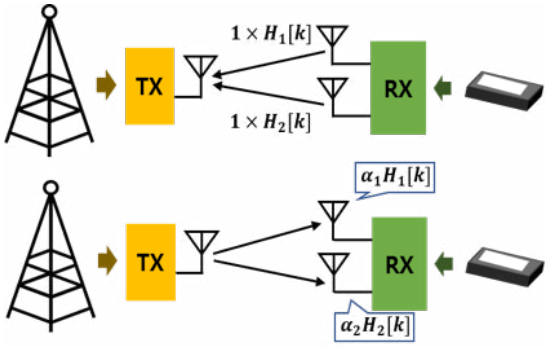

Fig. 1. SFLC-OFDM signal model assuming uplink and downlink channel asymmetry.

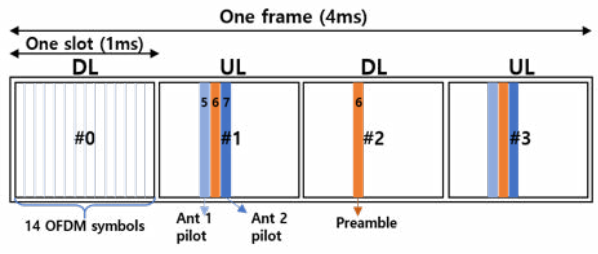

Fig. 2. TDD frame structure of SFLC-OFDM system

This model shows that signals in DL are received differently, reflecting both the asymmetry between UL and DL and the asymmetry between antennas. It defines the channel amplitude ratio between UL and DL for i-th antenna as α_i, where $\alpha_i \in \mathbb{R}$ with $\mathbb{R}$ denoting the set of real numbers. Here, the UL channel between and the TX antenna and the i-th RX antenna for the k-th subcarrier is defined as $H_i[k]$ which is a complex number. The DL channel is defined as $\alpha_i H_i[k]$, where α_i is a multiplier of $H_i[k]$. If α_1 and α_2 have different values, this represents the asymmetry between antennas.

To consider CSIT, we use a TDD frame structure, as illustrated in Fig. 2. Each frame consists of 4 slots, with UL and DL slots alternating in a 1:1 ratio in the time domain. The length of each slot is 1ms, and each slot consists of 14 OFDM symbols in the time domain. Each symbol is transmitted within a frame that has 1024 subcarriers. The TX transmits preamble symbols in the sixth OFDM symbol of every DL slot for DL synchronization. The RX transmits Channel Sounding Blocks (CSBs) in the fifth, sixth, and seventh OFDM symbols of every UL slot.

The CSB consists of preamble symbols for UL synchronization and pilot symbols for channel estimation. The preamble symbols are allocated to the subcarriers of the sixth OFDM symbol and are transmitted via the first antenna of the RX. We use an M-sequence with a length of 127 in the frequency domain for preamble signals, which is mapped onto 127 subcarriers for transmission. The pilot symbols for the first and second antennas are allocated to the fifth and seventh OFDM symbols, respectively.

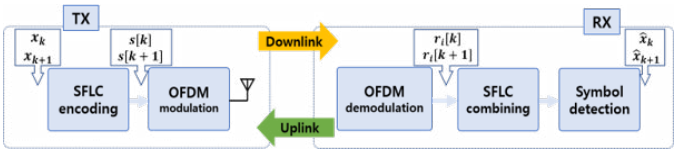

Fig. 3. Baseband Signal Processing in the SFLC-OFDM System

B. The System Model of SFLC System

The baseband signal processing model for SFLC is similar to that in an STLC system [21]. Unlike the STLC principle, which transmits a pair of symbols in continuous time, the SFLC system transmits a pair of symbols in the continuous frequency domain at k and $k+1$. Fig. 3 depicts the signal processing flow of the SFLC-OFDM system.

We denote X_k as the k-th data symbol generated from input bit. The TX encodes X_k and X_{k+1} into SFLC symbols, denoted by $S[k]$ and $S[k+1]$, based on the CSIT. We assume that the encoded pairs are mapped to consecutive subcarriers during OFDM modulation. Hence, $S[k]$ and $S[k+1]$ are allocated to the k-th and $(k+1)$-th subcarriers, respectively. Hence, SFLC encoding generates $S[k]$ and $S[k+1]$ as follows:

$$\begin{bmatrix} S^*[k] \\ S[k+1] \end{bmatrix} = \begin{bmatrix} \hat{H}_1[k] & \hat{H}_2[k] \\ \hat{H}_2^*[k] & -\hat{H}_1^*[k] \end{bmatrix} \begin{bmatrix} X_k \\ X_{k+1} \end{bmatrix}, \tag{1}$$

where $\hat{H}_i[k]$ represents the estimated channel between the TX antenna and the i-th RX antenna at the k-th subcarrier. The encoding algorithm in (1) assumes that the coherent bandwidth is larger than the frequency difference between two consecutive subcarriers and that $\hat{H}_i[k] = \hat{H}_i[k+1]$.

After OFDM demodulation, the RX obtains the received symbols of k-th subcarrier at the i-th antenna, denoted by $R_i[k]$. The received symbols are expressed as follows:

$$\begin{bmatrix} R_1[k] & R_1[k+1] \\ R_2[k] & R_2[k+1] \end{bmatrix} = \begin{bmatrix} H_1[k] \\ H_2[k] \end{bmatrix} \begin{bmatrix} S[k] & S[k+1] \end{bmatrix} + \begin{bmatrix} Z_1[k] & Z_1[k+1] \\ Z_2[k] & Z_2[k+1] \end{bmatrix}. \tag{2}$$

Here, $z_i[k]$ represents the Additive White Gaussian Noise (AWGN) corresponding to the i-th RX antenna and the k-th subcarrier. Then, the SFLC yields $\hat{X}_k$ and $\hat{X}_{k+1}$ through linear combinations as follows:

$$\begin{bmatrix} \hat{X}_k \\ \hat{X}_{k+1} \end{bmatrix} = \begin{bmatrix} R_1^*[k] + R_2[k+1] \\ R_2^*[k] - R_1[k+1] \end{bmatrix}. \tag{3}$$

The decoded symbols can be observed by substituting (1) and (2) into (3) as follows:

$$\begin{aligned} \hat{X}_k &= R_1^*[k] + R_2[k+1] \\ &= H_1^* S^*[k] + H_2 S[k+1] + Z_1^*[k] + Z_2[k+1] \\ &= H_1^*(H_1 X_k + H_2 X_{k+1}) + H_2(H_2^* X_k - H_1^* X_{k+1}) \\ &\qquad + Z_1^*[k] + Z_2[k+1] \\ &= (|H_1|^2 + |H_2|^2) X_k + Z_1^*[k] + Z_2[k+1], \end{aligned} \tag{4}$$

$$\begin{aligned} \hat{X}_{k+1} &= R_2^*[k] - R_1[k+1] \\ &= H_2^* S^*[k] - H_1 S[k+1] + Z_2^*[k] - Z_1[k+1] \\ &= H_2^*(H_1 X_k + H_2 X_{k+1}) - H_1(H_2^* X_k - H_1^* X_{k+1}) \\ &\qquad + Z_2^*[k] - Z_1[k+1] \\ &= (|H_1|^2 + |H_2|^2) X_{k+1} + Z_2^*[k] - Z_1[k+1]. \end{aligned} \tag{5}$$

When the signal strength is relatively strong compared to the noise, the phases of $\hat{X}_k$ and $\hat{X}_{k+1}$ are consistent with those of the original symbols. In this case, the RX can easily recover the data bits using maximum likelihood detection.

C. Recovery of Channel Phase Reciprocity

To facilitate CSIT for encoding, the SFLC-OFDM system needs to recover channel reciprocity. In terms of phase, we assume that the TX and RX address channel asymmetry by compensating for Symbol Timing Offset (STO), Carrier Frequency Offset (CFO) and Sampling Clock Offset (SCO) [20] based on the preamble. We denote $P[n]$ as the transmitted time-domain preamble signal of length N and $R_P[n]$ as the received time-domain signal containing the preamble. If the estimated STO and CFO are denoted by $\hat{\delta}$ and $\hat{\epsilon}$, respectively, the TX and RX are assumed to use estimation algorithms expressed as follows:

$$\hat{\delta} = \arg\max_{\delta \in \mathbb{N}} \Xi[\delta], \tag{6}$$

$$\hat{\epsilon} = \frac{\langle \Psi_0^* \Psi_1 \rangle}{\pi}, \tag{7}$$

where

$$\Xi[\delta] \triangleq \left| \sum_{n=0}^{N-1} R_P[\delta + n] P^*[n] \right|, \tag{8}$$

$$\Psi_i \triangleq \sum_{n=\frac{Ni}{2}}^{\frac{N(i+1)}{2}-1} \phi_{\hat{\delta}}(n), \tag{9}$$

$$\phi_{\hat{\delta}}(n) = R_P[\hat{\delta} + n] P^*[n]. \tag{10}$$

The algorithm in (6) and (8) derives the STO based on the auto-correlation between the received signal and $P[n]$. The algorithm in (7), (9) and (10) calculates the CFO based on the phase difference of the channel impulse response estimated from the received preamble signal.

For more accurate handling of the CFO, the system is assumed to leverage an additional estimation algorithm in the frequency domain. The rate of phase rotation due to SCO, denoted by $\Delta\beta$, is defined as follows:

$$\triangle\hat{\beta} = \frac{\langle \left(\frac{\chi_0}{K-1}\right)^* \left(\frac{\chi_1}{K-1}\right) \rangle}{2\pi \frac{K}{N}}, \tag{11}$$

where

$$\chi_i \triangleq \sum_{k=(i-1)K+1}^{iK-1} R_{\mathrm{p}}[k] P^*[k] \tag{12}$$

where $R_p[k]$ and $P[k]$ are the received and transmitted preamble symbols in the frequency domain, respectively.

III. Recovery of Channel Amplitude Reciprocity

Even if fine signal processing is carried out by correcting channel phase symmetry in the previous section, the estimated channel may mismatch with the actual channel that the received symbols experience. This generates unexpected phase rotation during SFLC decoding, causing the decoded symbols to have phase errors. Hence, we investigate the estimation of phase error by analyzing the transmission and reception processes from an analytical perspective.

A. Design of a Gain Imbalance Estimator

Based on our channel asymmetric model, the received symbols in (2) can be derived as follows:

$$\begin{bmatrix} R_1[k] & R_1[k+1] \\ R_2[k] & R_2[k+1] \end{bmatrix} = \begin{bmatrix} \alpha_1 H_1[k] \\ \alpha_2 H_2[k] \end{bmatrix} \begin{bmatrix} S[k] & S[k+1] \end{bmatrix} + \begin{bmatrix} Z_1[k] & Z_1[k+1] \\ Z_2[k] & Z_2[k+1] \end{bmatrix}. \tag{13}$$

The received symbols are linearly combined according to (3), resulting in $\hat{x}_k$ and $\hat{x}_{k+1}$ as follows:

$$\begin{aligned} \hat{X}_k &= \alpha_1 H_1^* S^*[k] + \alpha_2 H_2 S[k+1] + Z_1^*[k] + Z_2[k+1] \\ &= (\alpha_1 |H_1|^2 + \alpha_2 |H_2|^2) X_k + (\alpha_1 - \alpha_2) H_1^* H_2 X_{k+1} \\ &\quad + Z_1^*[k] + Z_2[k+1], \end{aligned} \tag{14}$$

$$\begin{aligned} \hat{X}_{k+1} &= \alpha_2 H_2^* S^*[k] - \alpha_1 H_1 S[k+1] + Z_2^*[k] - Z_1[k+1] \\ &= (\alpha_1 |H_1|^2 + \alpha_2 |H_2|^2) X_{k+1} - (\alpha_1 - \alpha_2) H_1 H_2^* X_k \\ &\quad + Z_2^*[k] - Z_1[k+1]. \end{aligned} \tag{15}$$

Compared with (4) and (5), (14) and (15) contain additional terms with non-zero phases. These terms cause $\hat{X}_k$ and $\hat{X}_{k+1}$ to have different phases from X_k and X_{k+1}. The additional terms share a common factor denoted by ϕ_α as follows:

$$\phi_\alpha = (\alpha_1 - \alpha_2) H_1^* H_2. \tag{16}$$

ϕ_α can be considered as an amplitude asymmetry factor. It is proportional to the difference between α_1 and α_2. ϕ_α reflects the extent of amplitude asymmetry between DL and UL channels. Thus, we can observe from (4) and (5) that channel amplitude asymmetry introduces unexpected phase rotation in the SFLC decoded symbols. It is noted that the phase rotation at the SFLC decoder does not occur if $\alpha_1 = \alpha_2$. The phase rotation becomes more significant as the difference in channel asymmetry for antenna 1 and 2 increases.

To prevent the phase rotation, it is necessary to restore channel amplitude reciprocity so that $(\alpha_1 - \alpha_2)$ in ϕ_α approaches 0. This requires an estimator for $(\alpha_1 - \alpha_2)$, which we will derive from the following definitions:

$$\alpha_1 - \alpha_2 = \Delta\alpha, \quad H_1 H_2^* = \theta_H. \tag{17}$$

Substituting (17), $\hat{x}_k$, $\hat{x}_{k+1}$ can be rewritten in a simpler form as follows:

$$\hat{X}_k = (\alpha_1 |H_1|^2 + \alpha_2 |H_2|^2) X_k + \Delta\alpha \theta_H X_{k+1}, \tag{18}$$

$$\hat{X}_{k+1} = (\alpha_1 |H_1|^2 + \alpha_2 |H_2|^2) X_{k+1} - \Delta\alpha \theta_H^* X_k. \tag{19}$$

Multiplied by X_{k+1} and X_k, respectively, (18) and (19) are further changed as follows:

$$\hat{X}_k X_{k+1} = (\alpha_1 |H_1|^2 + \alpha_2 |H_2|^2) X_k X_{k+1} + \Delta\alpha \theta_H X_{k+1}^2, \tag{20}$$

$$\hat{X}_{k+1} X_k = (\alpha_1 |H_1|^2 + \alpha_2 |H_2|^2) X_{k+1} X_k - \Delta\alpha \theta_H^* X_k^2. \tag{21}$$

The difference between (20) and (21), denoted by $\Lambda_{\Delta\alpha}$, is derived as follows:

$$\begin{aligned} \Lambda_{\Delta\alpha} &= \hat{X}_k X_{k+1} - \hat{X}_{k+1} X_k \\ &= \Delta\alpha \theta_H X_{k+1}^2 + \Delta\alpha \theta_H^* X_k^2. \end{aligned} \tag{22}$$

The goal of the estimator design can be achieved using (22). The estimator of $\Delta\alpha$, denoted by $\hat{\alpha}$, can be defined based on (22) as follows:

$$\begin{aligned} \hat{\alpha} &= \frac{\Lambda_{\Delta\alpha}}{X_{k+1}^2 + X_k^2} \\ &= \frac{\Delta\alpha \theta_H X_{k+1}^2 + \Delta\alpha \theta_H^* X_k^2}{X_{k+1}^2 + X_k^2}. \end{aligned} \tag{23}$$

We denote this estimator as Phase Rotation Offset (PRO), as unexpected phase rotation occurs in the decoded symbols when $\hat{\alpha}$ is non-zero.

The PRO can be derived only when the denominator of (23) is zero, depending on the X_k and X_{k+1}. For example, in the case of QPSK($M = 4$), the PRO is simplified as follows:
1) if $X_{k+1}^2 + X_k^2 = 4j$,

$$\hat{\alpha} = \frac{\Delta\alpha \theta_H \cdot 2j + \Delta\alpha \theta_H^* \cdot 2j}{4j} = \frac{1}{2} \Delta\alpha (\theta_H + \theta_H^*) \tag{24}$$

2) if $X_{k+1}^2 + X_k^2 = -4j$,

$$\hat{\alpha} = \frac{\Delta\alpha \theta_H \cdot (-2j) + \Delta\alpha \theta_H^* \cdot (-2j)}{-4j} = \frac{1}{2} \Delta\alpha (\theta_H + \theta_H^*) \tag{25}$$

Under the assumption of using the channel reciprocity recovery algorithms discussed in Section II.C, the phases of H_1 and H_2 are nearly zero. This implies that the real part of θ_H is positive and the phase of $(\theta_H + \theta_H^*)$ is zero. To this end, we can conclude that PRO is proportional to $\Delta\alpha$ and can represent it effectively.

B. Data-aided Gain Calibration

Based on the derivation in the previous section, we design a data-aided calibration, which is summarized as pseudo-code in Algorithm 1. To suppress noise effects, a moving average filter is applied to multiple decoded symbol pairs. This contributes to making the estimator more robust and improving the stability of the algorithm.

Based on the estimator output, RX performs gain calibration by adjusting the receive gain of a RF chain for each antenna. If PRO is estimated as a positive value, RX can either increase the receive gain of antenna 2 or decrease the receive gain of antenna 1. Conversely, if the estimated PRO is negative, the UE adjusts the received gain in the opposite manner. This gain calibration can approach the PRO to zero in a delicate way.

Algorithm 1 Pseudo Code for the Proposed Data-Aided Gain Calibration Method

1. Calculate $\Lambda_{\Delta\alpha}$ according to (22).

2. Obtain $\hat{\alpha}[n]$ according to (23) if $x_{k+1}^2 + x_k^2$ is non-zero.

3. Perform moving averaging with multiple PROs as follows:
$\hat{\phi}_{\alpha[n+1]} = a\hat{\phi}_{\alpha[n]} + (1-a)\hat{\phi}_{\alpha}$,
where $a \in [0, 1)$ is a moving averaging constant.

4. Adjust the receive gain for gain calibration as follows:
if $\hat{\phi}_{\alpha n+1} > 0$ **then**
Increase the receive gain of the RF chain for antenna 2.
else if $\hat{\phi}_{\alpha n+1} < 0$ **then**
Decrease the receive gain of the RF chain for antenna 2.
end if

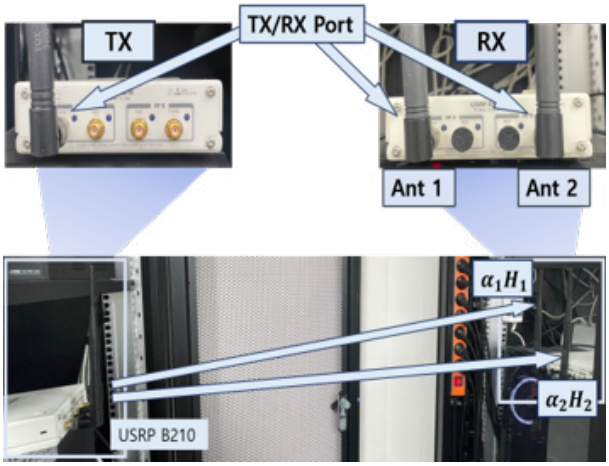

Fig. 4. SFLC-OFDM testbed with USRPs

IV. Implementation and Experiment Results

To evaluate the performance of the proposed gain imbalance calibration in practical environments, we implement the algorithm on a software modem. We build a USRP-based testbed which operates in real-time. As shown in Fig. 4, we connect one antenna to the transmitting USRP and two antennas to the receiving USRP to configure the 1x2 SFLC system. To ensure channel symmetry with identical DL and UL channel paths, the antennas are connected to the TX/RX port of the USRP, allowing for simultaneous transmission and reception. The detailed experimental parameters are set as shown in Table I.

A. Stability of the PRO estimator

To assess the stability of the PRO estimation, we observe how the instantaneous values of the estimated PRO vary. For each experiment, we change α_2 by applying an RX gain offset to the 2nd antenna. The offset that reduces the magnitude of α_2 is simply defined as β. As β increases, the α_2 decreases, leading to greater channel asymmetry. The PRO

TABLE I
Experiment Parameters

Center Frequency	**3.3GHz**	**Sampling Rate**	**15.36MHz**
Subcarrier Spacing	**15kHz**	**FFT Size**	**1024**
Bandwidth	**10MHz**	**Modulation Scheme**	**QPSK**
RF device	**USRP B210**	**CPU**	**Core-i9**

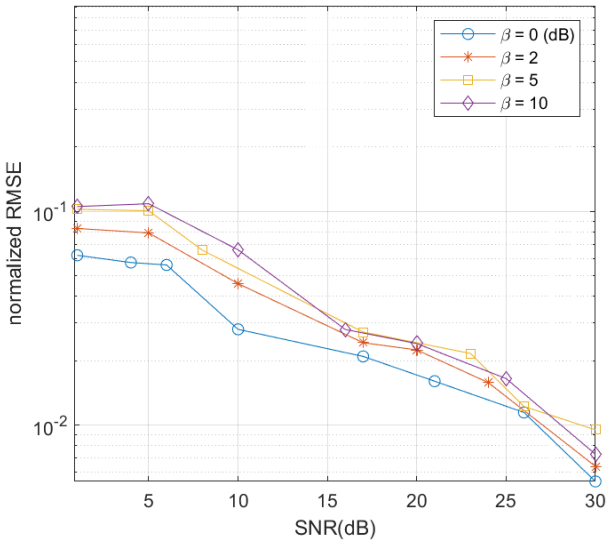

Fig. 5. N-RMSE of moving average of PRO versus SNR according to α_2

estimation error was calculated based on the Normalized Root Mean Square Error (N-RMSE). N-RMSE was calculated by comparing the instantaneous PRO values with the estimated PRO when the Signal to Noise Ratio (SNR) is above 30dB.

Fig. 5 shows the N-RMSE in terms of SNR, proving that the PRO estimation functionally works in various environments. The results indicate that when SNR is 25dB or higher, the N-RMSE is derived below 0.02. When SNR is between 15dB and 25dB, the N-RMSE ranged from 0.02 to 0.04, demonstrating the relatively stable performance of PRO estimation. However, when SNR is below 15dB, the N-RMSE increases significantly. The proposed estimator is designed to be effective specifically in high SNR environments because the primary goal is to enhance performance under good signal conditions where channel symmetry has the most impact. The focus is on improving performance when the signal is strong, so the effectiveness at SNR levels above 15 dB is intentional and aligned with this objective.

Additionally, as the asymmetry in channel amplitude becomes more severe, the stability of the PRO estimation deteriorates notably in weak signal environments. This can be improved by adjusting the moving average constant. Increasing a will help the PRO estimation obtain stable results when received signal strength is weak or when channel asymmetry is significantly large. Hence, a needs to be carefully configured, taking into account the target channel environment.

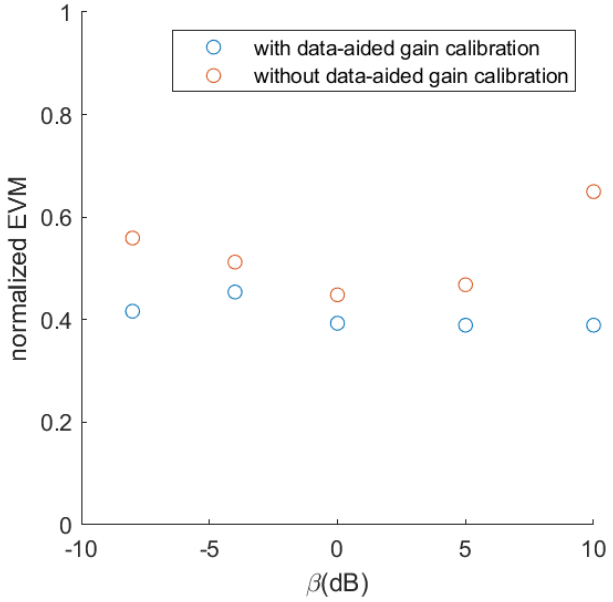

Fig. 6. EVM before and after channel imbalance calibration

B. The Performance of Data-Aided Gain Calibration

Subsequently, we conduct the data-aided gain calibration to verify its effectiveness. We observe the Error Vector Magnitude (EVM) of the decoded symbols [20]. After decoding SFLC symbols, the RX measures and presents the EVM between decoded symbols and transmitted symbols. This EVM is measured by varying the bias and magnitude of the β. Fig. 6 illustrates the normalized EVM before and after data-aided gain calibration. The values represent a ratio of EVM in the range of (0,1). We can see that the overall EVM is improved with the implied calibration. The EVM is further improved as the β increases and channel asymmetry becomes severe. We can also see that EVM is improved even when the β is 0, demonstrating the achievement of delicate recovery of channel amplitude reciprocity. The results demonstrate that not only is the calibration functioning, but also the proposed scheme accurately recovers channel symmetry.

V. Conclusions

This paper addresses performance degradation in TDD-based SFLC-OFDM systems due to channel amplitude asymmetry. We design an estimator to correct unexpected phase rotation and propose a gain calibration to resolve the asymmetry. Experimental results using a USRP-based testbed demonstrate the stability of the PRO estimator and its effectiveness in reducing phase rotation. The proposed algorithm eliminates the need for additional reference signals and shows potential for application in both MxN STLC and massive MIMO systems.

References

[1] S. Yang and L. Hanzo, "Fifty Years of MIMO Detection: The Road to Large-Scale MIMOs," *IEEE Communications Surveys & Tutorials*, vol. 17, no. 4, pp. 1941–1988, 2015.

[2] P. K. S. S. Kurma, K. Singh and C. P. Li, "Outage Probability Analysis of Uplink Cell-Free Massive MIMO with User Mobility," *IEEE Military Communications Conference (MILCOM)*, pp. 37–42, 2022.

[3] M. A. Albreem, M. Juntti, and S. Shahabuddin, "Massive MIMO Detection Techniques: A Survey," *IEEE Communications Surveys & Tutorials*, vol. 21, no. 4, pp. 3109–3132, 2019.

[4] L. Lu, G. Y. Li, A. L. Swindlehurst, A. Ashikhmin, and R. Zhang, "An Overview of Massive MIMO: Benefits and Challenges," *IEEE Journal of Selected Topics in Signal Processing*, vol. 8, no. 5, pp. 742–758, 2014.

[5] J. Tan and L. Dai, "Channel Feedback in TDD Massive MIMO Systems With Partial Reciprocity," *IEEE Transactions on Vehicular Technology*, vol. 70, no. 12, pp. 12 960–12 974, 2021.

[6] H. Yin and D. Gesbert, "A Partial Channel Reciprocity-Based Codebook for Wideband FDD Massive MIMO," *IEEE Transactions on Wireless Communications*, vol. 21, no. 9, pp. 7696–7710, 2022.

[7] E. Becirovic, E. Björnson, and E. G. Larsson, "Reciprocity Aided CSI Feedback for Massive MIMO," *2020 54th Asilomar Conference on Signals, Systems, and Computers*, vol. 00, pp. 1022–1027, 2020.

[8] H. P. H. Son, G. Kwon and J. S. Park, "Impact of Imperfect Channel State Information on Achievable Rate With Zero-Forcing Precoding in Massive MIMO Systems for Multi-Numerology," *MILCOM 2023 - 2023 IEEE Military Communications Conference (MILCOM)*, pp. 89–94, 2023.

[9] M. Petermann, M. Stefer, F. Ludwig, D. Wubben, M. Schneider, S. Paul, and K.-D. Kammeyer, "Multi-User Pre-Processing in Multi-Antenna OFDM TDD Systems with Non-Reciprocal Transceivers," *IEEE Transactions on Communications*, vol. 61, no. 9, pp. 3781–3793, 2013.

[10] M. Guillaud, D. Slock, and R. Knopp, "A practical method for wireless channel reciprocity exploitation through relative calibration," *Proceedings of the Eighth International Symposium on Signal Processing and Its Applications, 2005.*, vol. 1, pp. 403–406, 2005.

[11] X. Jiang, M. Cirkic, F. Kaltenberger, E. G. Larsson, L. Deneire, and R. Knopp, "MIMO-TDD reciprocity under hardware imbalances: Experimental results," in *2015 IEEE International Conference on Communications (ICC)*, 2015, pp. 4949–4953.

[12] X. Jiang, A. Decurninge, K. Gopala, F. Kaltenberger, M. Guillaud, D. Slock, and L. Deneire, "A Framework for Over-the-Air Reciprocity Calibration for TDD Massive MIMO Systems," *IEEE Transactions on Wireless Communications*, vol. 17, no. 9, pp. 5975–5990, 2018.

[13] J. Shi, Q. Luo, and M. You, "An Efficient Method for Enhancing TDD Over the Air Reciprocity Calibration," *2011 IEEE Wireless Communications and Networking Conference*, pp. 339–344, 2011.

[14] Q. Liu, X. Su, J. Zeng, L. Liu, and T. Lv, "Antenna Calibration Method for MMSE-Based Network MIMO System," *2015 IEEE/CIC International Conference on Communications in China - Workshops (CIC/ICCC)*, pp. 120–125, 2015.

[15] B. Akan, E. Ekici, L. Qiu, A. C. Snoeren, C. Shepard, H. Yu, N. Anand, E. Li, T. Marzetta, R. Yang, and L. Zhong, "Argos: Practical Many-Antenna Base Stations," *Proceedings of the 18th annual international conference on Mobile computing and networking*, pp. 53–64, 2012.

[16] S. Han, C. Yang, G. Wang, D. Zhu, and M. Lei, "Coordinated Multi-Point Transmission Strategies for TDD Systems with Non-Ideal Channel Reciprocity," *IEEE Transactions on Communications*, vol. 61, no. 10, pp. 4256–4270, 2013.

[17] J. Geng, Z. Wei, X. Wang, X. Liu, W. Xiang, and D. Yang, "On Antenna Calibration for the TDD-based Network MIMO System," *2013 IEEE International Conference on Communications (ICC)*, pp. 5866–5871, 2013.

[18] N. Torkzaban, M. A. A. Khojastepour, and J. S. Baras, "Channel Reciprocity Calibration for Hybrid Beamforming in Distributed MIMO Systems," *2023 IEEE Wireless Communications and Networking Conference (WCNC)*, vol. 00, pp. 1–6, 2023.

[19] J. Vieira and E. G. Larsson, "Reciprocity calibration of Distributed Massive MIMO Access Points for Coherent Operation," *2021 IEEE 32nd Annual International Symposium on Personal, Indoor and Mobile Radio Communications (PIMRC)*, vol. 00, pp. 783–787, 2021.

[20] S. Kim, H.-G. Lee, S. Lee, J. Kim, J. Joung, and J. Kim, "Single-User SFLC-OFDM System Realization Based on Channel Reciprocity Recovery," *IEEE Access*, vol. 11, pp. 109 082–109 094, 2023.

[21] J. Joung, "Space–Time Line Code," *IEEE Access*, vol. 6, pp. 1023–1041, 2018.

[22] J. Joung, J. Choi, and B. C. Jung, "Double Space–Time Line Codes," *IEEE Transactions on Vehicular Technology*, vol. 69, no. 2, pp. 2316–2321, 2020.